Journal of Korean Vacuum Science & Technology; JKVST
Vol. 4, No. 3, October 2000, pp. 68~72

The study of the c(2×2) ordered Mn surface alloy Pd(001)

J. W. Jung, S. H. Kim,* C. Y. Park* J. K. Seo, H. G. Min, D. H. Byun, and J. S. Kim*****

Department of Physics, Hongik University, Seoul 121-791, Korea
**Department of Physics, Sungkyunkwan University, Suwon 440-746, Korea*
***Department of Ophthalmic Optics, Chodang University, Muan 534-701, Korea*
****Department of Physics, Sookmyung Women's University,140-742 Seoul, Korea*
(Received July 13, 2000)

Abstract – We have deposited Mn on Pd(001) at RT up to 30 ML. LEED pattern changed from p(1×1) to c(2×2) order below 0.5 ML Mn deposition. During Mn deposition, we have not found any changes in the peak position and the intensity of LEED I/V curve. Using LEED I/V curve analysis for each coverage, we found atomic structure and surface composition of c(2×2) ordered Mn alloy on Pd(001) surface. Above 1 ML Mn, in the first layer the Mn subplane lies above the Pd subplane by 0.32 Å. This result is very different from the earlier result of Jona et al., who contended that after annealing at 200 for 2 min, a buckled first layer with the Mn subplane lower than the Pd subplane by 0.2 Å.

I. Introduction

Ultrathin magnetic films on nonmagnetic metal substrates are very interesting model systems of two-dimensional magnetism in as respect of salient magnetic features such as magnetic overlayers with highly enhanced magnetic moments, magnetically dead layer, and perpendicular magnetic anisotropy [1]. Furthermore, metastable nature of thin magnetic films allows the realization of the atomic structures of thin films, which is not found in nature as bulk. For example, Prinz stabilized bcc Co on a (110) substrate of fcc GaAs at room temperature by molecular-beam epitaxy (MBE) [2]. Such a metastable structure may be used to tailor novel magnetic properties.

Mn shows a large variety in structural and magnetic properties. A cubic α-phase with 58 atoms in a unit cell is stable up to 727°C: a cubic β-phase with 20 atoms/cell, stable in between 727 and 1095°C: a face-centered cubic γ-phase , stable in between 1095 and 1133°C: a body-centered cubic δ-phase, stable between 1133°C and 1244°C which is the melting point of Mn [3].

The magnetic moment of Mn depends on its atomic structure [4], and the stabilization of γ- and δ- phase by epitaxy has been attempted by a few authors. Heinrich *et al.* [5] have grown Mn films on Ru(0001), Ni(001), Fe(001) and reported the formation of complex phases on the two substrates (Ru, Ni). From the structure of the substrate Fe(001), he inferred that bcc Mn would grow on an Fe(001).

S. Blugel *et al.* [6] predicted a c(2×2) antiferromagnetic structure of Mn on Fe(001) through full potential linearized augemented planewave potentials (FLAPW) calculation.

J. Khalief [7] has shown that in plane ferromagnetic p(1×1) and c(2×2) superstructure are stable for 1 ML Mn film and layer-antiferromagnetic solution is more stable for all thickness of Mn films thicker than 1 ML on Pd(001). The surface free energy of Mn (2.12 J/m_2) (1) is larger than that of Pd(1.90 J/m_2) [8]. So it is expected that Pd atoms may form a layer on top of the deposited Mn film on Pd(001) surface or the Pd atoms may form a surface alloy with Mn atoms.

By low energy electron diffraction (LEED) I/V (spot intensity vs beam energy) analysis, D. Tian *et al.* [9] have suggested that the c(2×2) Mn on Pd(001) surface at room temperature (RT) is equivalent to the (001) surface of ordered Pd_3Mn bulk alloy. The first layer is 50%-50% mixture of Mn and Pd, the second layer consists of Pd, and the third layer has the same composition as the first layer. However, their reliability factor (R-value) was so large. They could not pin down correct surface structure and composition of each layer.

In this paper, the atomic structure of the c(2×2) ordered Mn surface alloy on Pd(001) was studied to clarify their atomic structures after deposition of Mn on Pd(001) at RT with LEED I/V analysis.

II. Experiments

All the experiments were performed in an ultrahigh vacuum chamber (TNB-X series, Perkin Elemer Corp) with base pressures of 3×10^{-11} torr. The Pd(001) single crystal sample was a "top-hat" shaped disk whose diameter was 8 mm and the thickness was 1 mm. The sample was wrapped and mounted with a thin Ta foil. The sample temperature was monitored by a chromel-alumel thermocouple attatched to the Ta foil.

A clean Pd surface was prepared by repeated cycles of sputtering with Ar^+ ion of 2 keV incidence energy, and followed annealing up to 1200 K until no contaminants such as C and O were detected by an Auger electron spectrometer (AES) with a cylindrical mirror analyzer (CMA, Perkin Elemer Corp). To eliminate the residual C contamination, the sample was heated up to 1200 K in an 1×10^{-7} torr of oxygen pressure.

To check the cleanness of Pd sample, we used the shape and the ratio of Pd 279 eV (transition energy) to Pd 333 eV peaks, which was about 0.19 for a clean Pd(001) surface, because C peak (272 eV) is very close to a Pd peak (279 eV).

The clean Pd(001) surface showed a sharp (1×1) LEED pattern with low background intensity. Mn was thermally evaporated from a Mn chip (99.95%) that was wound around by a tungsten filament. The deposition rate was 11.5 ML per minute. During the evaporation, the chamber pressure was kept below $3\sim4\times10^{-10}$ torr, and the sample temperature was around 300 K. The Mn deposition was monitored with a quartz microbalance and was calibrated by the intensity ratio of the AES peaks with their transition energies of 592 eV for Mn and 333 eV for Pd. For the calibration, We used Seah's empirical equation for escape depths of Pd (333 eV) and Mn (522 eV) peaks [10]. The mean free paths are 7.67 Å for Mn (592 eV), 5.67 Å for Pd(333 eV). LEED I/V data was collected by employing a video LEED system built in our laboratory [11]. All the LEED I/V data was taken with the incident beam normal to surface. The residual magnetic field was kept below 0.05 G in all three perpendicular direction by employing three perpendicular Helmholtz coils. The I/V curve of several symmetrically inequivalent beams were taken and then averaged before data analysis

III. Results and Discussion

First, we checked atomic structure of a clean Pd(001) surface. The analysis of LEED I/V characteristics were made with TLEED (tensor LEED) algorithm [12]. Scattering phase shifts for the angular momentum quantum number l up to 6 were used and thermal vibration effects were taken into account by Debye-Waller factor with Debye temperature of 274 K for Pd. The best fit between theory and experiment was achieved by minimizing the Pendry R factor (R_p) and the error bar in the structure determination is assessed by its variance.

For the clean Pd(001) surface, the analysis was done by varying the first d_{12}, the second d_{23}, and the third d_{34} interlayer spacing. Interlayer distance of bulk Pd(001) is 1.945 Å, and the best fit to the experimental results was found for $\Delta d_{12} = -0.013$ Å and $\Delta d_{23} = -0.006$ Å, $\Delta d_{34} = -0.013$ Å from the bulk spacing with $R_P = 0.2772$. For all the calculations, in-plane lattice constant was kept at the bulk Pd value of 2.75A.

We deposited Mn on Pd(001) at RT up to 30 ML. With increasing Mn coverage, LEED pattern changed from p(1×1) to c(2×2) order below 0.5 ML Mn deposition. Background intensity increased slightly with further Mn deposition but the c(2×2) pattern remained up to 7 ML. Above 7 ML, LEED pattern was still p(1×1) on visual inspection. However, even at 30 ML Mn coverage, very faint c(2×2) pattern was still observed at low energy range, and Pd AES signal was detected. After brief annealing of the sample at 150°C for 5 min, AES ratio of Mn to Pd signal changed from 14.25 to 8, and the sharper c(2×2) LEED pattern appeared with decreased background intensity. From the LEED pattern for the clean Pd and for 30 ML Mn at the same incident energy, it is clear that distance between the beams is same, which says Mn films grows pseudomorphically.

For 0.5 ML, 2 ML, 3 ML Mn films deposited on Pd(001) at room temperature and annealed at 150°C for 5 min, LEED I/V curves were obtained from four symmetrically equivalent beams including a (1/2,1/2) beam between 40-400 eV by a fully automated video

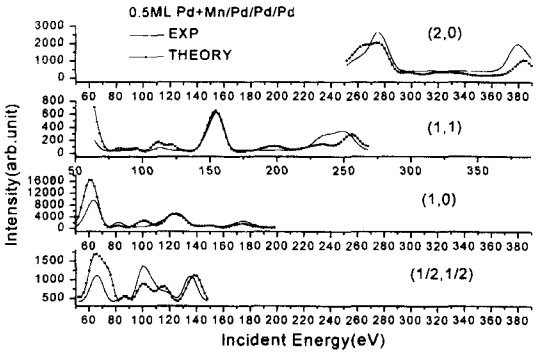

Fig. 1. The best fit spectra of annealed 0.5 ML Mn on Pd(001).

LEED system. LEED I/V analysis was done by employing the tensor LEED program. For the thin film calibrated by AES as 0.5 ML Mn thick, we tried to fit our experimental curves for various growth models.

For 0.5 ML Mn, the optimum structure was found to be a surface alloy, the optimum R_p factor was 0.2534, and the model gives the right AES intensity ratio as observed in the experiment. The AES intensity ratio was predicted to be 0.05 in our calibration, and 0.04 in the experiment. Fig. 1 shows the best fit curve for the experimental one. The peak positions and intensity ratio are reasonably well reproduced. For the optimized structure, a small corrugation of 2.1% (0.04) between Mn atom and Pd atom in the first surface alloy layer is found. The interlayer spacing between 2nd and 3rd layer is contracted by a small amount, $\Delta d_{23} = -2.63\%$ (1.899), the interlayer spacing between 3rd and 4th layer is relaxed, $\Delta d_{34} = +6.3\%$ (2.068). Fig. 2 is the side view of the optimized structure for annealed 0.5 ML Mn on Pd(001) surface.

After 2 ML Mn film deposited, the optimum structure was found to be the 1 ML thick subsurface Mn film below severelly buckled Mn and Pd plane. In the first layer the Mn subplane lies above the Pd subplane by 0.32 Å (17%) and the interlayer spacing between 2nd and 3rd layer is relaxed by a small amount of 0.14 Å, compared to the Pd distance 1.945A. The interlayer spacing between 3rd and 4th layer is relaxed by a small amount of 0.075 Å (Fig. 3).

This result is very different from the earlier result of Jona *et al.* [10], who contended that after annealing at 200°C for 2 min, a buckled first layer with the Mn subplane lower than the Pd subplane by 0.2 Å. The second interlayer spacing is smaller by 0.1 Å relative

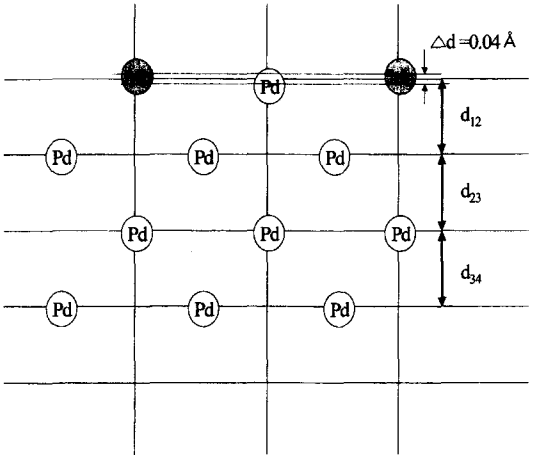

Fig. 2. Side view of the optimized structure for annealed 0.5 ML Mn on Pd(001).

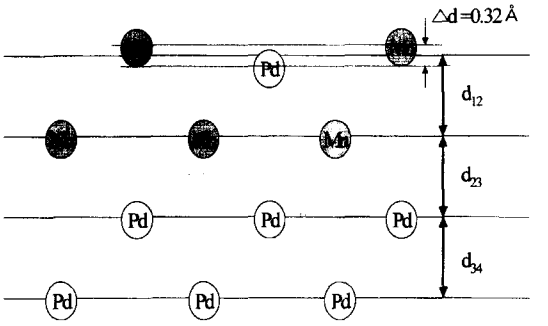

Fig. 3. Side view of the optimized structure for annealed 30 ML Mn on Pd(001).

to the Pd spacing.

For the case of 0.5 ML, Mn coverages estimated from the best fit structures which agree well with the coverage from quartz microbalance. The AES ratio from the structure agrees with the experimental AES ratio for Mn films below 1.5 ML. The experimental ratio equals to the calculated ratio 0.12 (in-plane alloy) for 1.5 ML Mn.

For 3 ML Mn, the thickness for the best fitted I/V result is different from the thickness calibrated by the quratz microbalance and the AES peak ratio. The LEED electrons employed in the current study have energies ranging from 40-400 eV and the energy of the AES electron has a $\lambda = 7.67$ Å for Mn(592 eV), $\lambda = 5.67$ for Pd(333 eV), respectively. Due to their short escape depths, they may not be detected if the Mn atom are deep inside the bulk.

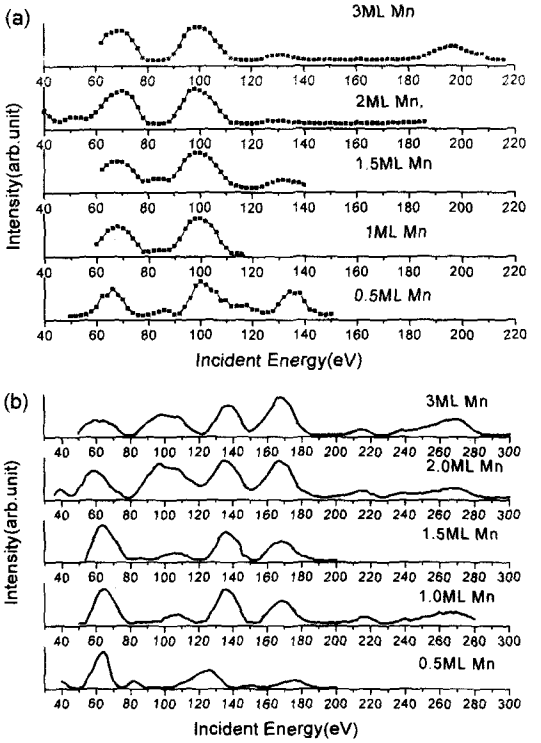

Fig. 4. I/V curve as a function of Mn thickness (a) (1/2, 1/2)beam, (b) (1,0)beam.

Fig. 4 shows I/V curves as a function of Mn coverage. For (1/2,1/2) beam, very similar I/V curves are found for films from 0.5 ML to 3 ML Mn. It means that the c(2×2) surface alloy is a very stable structure. We expected that a small shift in the peak position is originated from the change of work-function and the element of surface region rather than the atomic structure. We has compared I/V curves between those before and after annealing. We have not found any change in the peak position and the intensity. We expected that the atomic structure and composition near the surface was not changed seriously before and after annealing.

For the case of 0.5 ML and 1 ML, experimental AES intensity ratios agree well with the calculated value based on the best structural model. The difference in ratios between before and after annealing the sample is not significant. It means that the alloy forms as soon as deposited on Pd(001) surface even at room temperature. Even, for the 3 ML case, the ratio difference between before and after annealing the sample was not found.

As we deposited 30 ML Mn on Pd(001) surface, very faint c(2×2) pattern still remained at low energy range and Pd AES signal remained until 30 ML in AES spectra. After brief annealing of the sample at 150 for 5 min, we have found a large change in AES ratio; Pd atom signal increased a lot and the sharper c(2×2) pattern appeared. It means that the Pd atom diffuse up to the surface to form a surface alloy.

The surface free energy of Mn (2.12 J/m_2) is larger than that of Pd (1.90 J/m_2), From the result we can expect the possibility of the interdiffusion of Mn and Pd atoms.

After 1ML Mn deposition, we have found large buckling. We could find such buckling for some other surface alloys such as 0.1 Å of Au/Cu(001) [13], 0.02 Å of Pd/Cu(001) [14]. Wu *et al.* [14] reported that the corrugation of the surface alloy layer increases with the increasing difference in the atomic radius of the alloy constitution. However, the buckling of 0.3 Å in Mn/Cu(001) [15] and of 0.25 Å in Mn/Ni(001) [16] are considerably larger than the buckling of the AuCu surface alloy. This showed that simple atomic size effects are insufficient to explain the buckling of surface alloys. Futher we would expect that the buckling should be slightly larger in Mn-Ni on Ni(001) surface than in Mn-Cu on Cu(001) by the atomic size difference. However, a larger buckling is found for the c(2×2) surface alloy Mn on Cu(001).

AuCu system is nonmagnetic system and Mn/Ni, Mn/Cu are magnetic system. Blugel *et al.* [17] reported that a marginal buckling of less than 0.02 Å is found for the paramagnetic surface alloy for the CuPd and CuAu system. For the ferromagnetic surface alloy, a buckling of 0.24 Å is found in the calculation which showed a good agreement with the experiment. According to the calculation the ferromagnetic surface alloy has a smaller minimum energy than the nonmagnetic surface alloy, and both the stability and corrugation are caused by the pronounced magnetic moment of the Mn atoms and the resulting gain in magnetic energy [18]. It is known from the many theoretical works for Mn that Mn atoms show large local magnetic moments. Various magnetic phases such as c(2×2) antiferromagnetic state or p(1×1) ferromagnetic state exist on surface and thin films. A lattice expansion should be accompanied by an increase in the magnetic moment.

IV. Summary

We deposited Mn on Pd(001) at RT up to 30 ML. LEED pattern changed from p(1×1) to c(2×2) order below 0.5 ML Mn deposition. During Mn deposition, we have not found any changes in the peak position and the intensity. We expected that the atomic structure and composition near the surface was not changed seriously before and after annealing.

After annealing 0.5 ML Mn deposited on Pd(001) substrate, a small corrugation of 2.1% (0.04 Å) between Mn atom and Pd atom in the first surface alloy layer is found. After 1 ML Mn, in the first layer the Mn subplane lies above the Pd subplane by 0.32 Å (17%). This result is very different from the earlier result of Jona *et al.* [9], who contended that after annealing at 200°C for 2 min, a buckled first layer with the Mn subplane lower than the Pd subplane by 0.2 Å. For 3 ML thickness, the optimum structure was found to be the 1 ML thick subsurface Mn film below as severally buckled Mn and Pd plane as for 2 ML film deposited.

Acknowledgements

This work was supported by the Korea Science and Engineering Foundation through the Atomic-scale Surface Science Research Center at Yonsei University.

References

[1] H. Dreysse and C. Demangeat, Surf. Sci. Rep. **28**, 65-122 (1997).
[2] G. A. Prinz, Phys. Rev. Lett., **54**, 1051 (1985).
[3] W. B. Pearson, "A handbook of Lattice Spacings and Structures of Metals and Alloys". Pergamon Press (1958, 1967).
[4] V. L. Moruzzi, P. M. Marcus, and P. C. Pattnaik, Phys. Rev. **B37**, 8003 (1988). P. Kruger, O. Elmouhssine, C. Demengeat, and J. C. Parlebas, Phys. Rev. **B54**, 6393 (1996).
[5] B. Heinrich, A. S. Arrott, C. Liu, and S. T. Purcell, J. Vac. Sci. Technol. **A5**, 1935 (1987).
[6] S. Brugel, B. Drittler, R. Zeller, and P. H. Dederichs, Appl. Phys. **A49**, 547 (1989).
[7] Jamil Khalife, J. Magn. Magn. Mater, **201-206**, 159 (1996).
[8] H. L. Skriver and N. M. Rosengaard, Phys. Rev. **B46**, 7157 (1992).
[9] D. Tian, R. F. Lin, F. Jona, and P. M. Marcus, Solid State Commun, **B74**, 1017 (1990).
[10] M. P. Seah and W. A. Dench : Surface and interface Analysis **1**, 2 (1976).
[11] S. H. Kim, et al., Phys. Rev. **B55**, 7904 (1997).
[12] J. Quinn, Y. S. Li, D. Tian, H. Li, and F. Jona, Phys, Rev. **B42**, 11348 (1990).
[13] Z. Q. Wang, Y. S. Li, C. K. C. Lok, J. Quinn, and F. Jona, Solid State Commun. **62**, 181 (1987).
[14] S. C. Wu, S. H. Lu, Z.Q. Wang, Y. S. Li, C. K. C. Lok, J. Quinn, D. Tian, and F. Jona, Phys. Rev. **B38**, 5363 (1988).
[15] T. Flores, M. Hansen, and M. Wuttig, Surf. Sci. **279**, 251 (1992).
[16] M. Wuttig, C. C. Knight, and T. Flores, Phys. Rev. **B48**, 251 (1993).
[17] S. Blugel, Appl. Phys. **A63**, 595-604 (1996).
[18] Blugel et.al. Phys. Rev. Lett., **70**, 3619 (1993).